Table 10. Symbol synchronizer and synthesizer settings

Operational parameters				Synthesizer settings		
Input symbol rate R, bits/s	Loop bandwidth %			Frequency range, MHz	Center frequency, Hz	24–MHz select sweep column
5.6–56	0.2	0.05	0.01	1	1600R	COL BB EXT
5.6–56	0.02	0.005	0.001	1	1600R	COL CC EXT
56–560	0.2	0.05	0.01	1	1600R	COL AA EXT
56–560	0.02	0.005	0.001	1	1600R	COL BB EXT
560–5600	0.2	0.05	0.01	1	160R	COL AA EXT
560–5600	0.02	0.005	0.001	1	160R	COL BB EXT
5600–56000	0.2	0.05	0.01		16R	COL AA EXT
5600–56000	0.02	0.005	0.001	1	16R	COL BB EXT
56000–250000	0.2	0.05	0.01	10	16R	COL AA EXT
56000–250000	0.02	0.005	0.001	10	16R	COL BB EXT

narrow the bandwidth in steps. One should wait a time equal to several inverse loop bandwidths, say $5/w_L$ seconds or more, before narrowing the bandwidth, so as to be fairly certain that the frequency and phase errors are small before switching. The phase window can be narrowed to $W = \frac{1}{8}$ at any time after initial acquisition.

d. Design changes. Only one significant design change has been made since the previous article. This change was the inclusion of a nonlinear digital low-pass smoothing filter for use with $w_L T = 0.2$ and 0.02% only. The purposes of the filter are to reduce sampling jitter at wide loop bandwidths and to reduce the dynamic range of the proportional control signal to the VCO by a factor of 4. Reduction in sampling jitter is especially significant at $w_L T = 0.2\%$ and with high symbol SNRs. Reduction in dynamic range allows the use of lower VCO gains and proportionally higher VCO control voltages, and hence reduces the possibility that system noise might have a significant effect on the VCO control signal.

This nonlinear filter will be described in detail in a future article.

2. Information Systems: A Binary-Coded Sequential Acquisition Ranging System, W. L. Martin

a. Introduction. In the past, ranging systems could be conveniently assigned to one of two classifications, depending upon their method of coding. First, there were the single-component systems, which utilized a pseudonoise (PN) code of sufficient period to resolve range ambiguities and a bit length short enough to provide the required resolution. Examples include lunar and planetary mapping systems where simplicity of design and acquisition procedure have been traded for relatively long acquisition times.

Second were the multi-component systems, which combined a group of short sequences into a code of the desired length. Examples are the *Apollo* Mark I, *Mariner* Venus 1967, *Mariner* Mars 1969, and *Sidetone* ranging systems where the intent was clearly to minimize the acquisition time.

It has been shown by Titsworth (Ref. 1) that the best acquisition time for a multi-component, single-correlator system is achieved when the individual component lengths v_i are

$$v_i \simeq n(p)^{1/2} \simeq e \tag{1}$$

where p is the combined code period and n is the number of components. Unfortunately, an additional constraint on PN coded systems demands that the individual component periods must all be relatively prime. Thus, the designer is forced to trade optimality for reality and select component lengths which best fit both criteria. Typical choices for component lengths include 2, 7, 11, 15, 19, 23, etc.

While offering a substantial reduction in acquisition time, the multi-component combinatorial units do suffer some degradation due to component sharing of the transmitted power (Ref. 1). This degradation can be overcome by sequentially transmitting components, one at a time, so that full transmitted power is available to each. For example, a 3-dB improvement is realized over combinational systems allocating 50% of the power to each component, and a 6-dB gain is realized over those assigning 25% to each component. Thus, it appears that the optimal system would sequentially transmit n components of length e.

b. A binary-coded sequential ranging machine. Figure 43 is a simplified block diagram of a binary-coded sequential acquisition ranging system. A frequency synthesizer generates f_s (nominally 22 MHz), which is multiplied by three and phase-modulated by the transmitter coder. The code is generated by dividing the 66-MHz output from the $\times 3$ multiplier by 64 and applying the result to an 18-stage binary counter. Each of the 18 outputs from

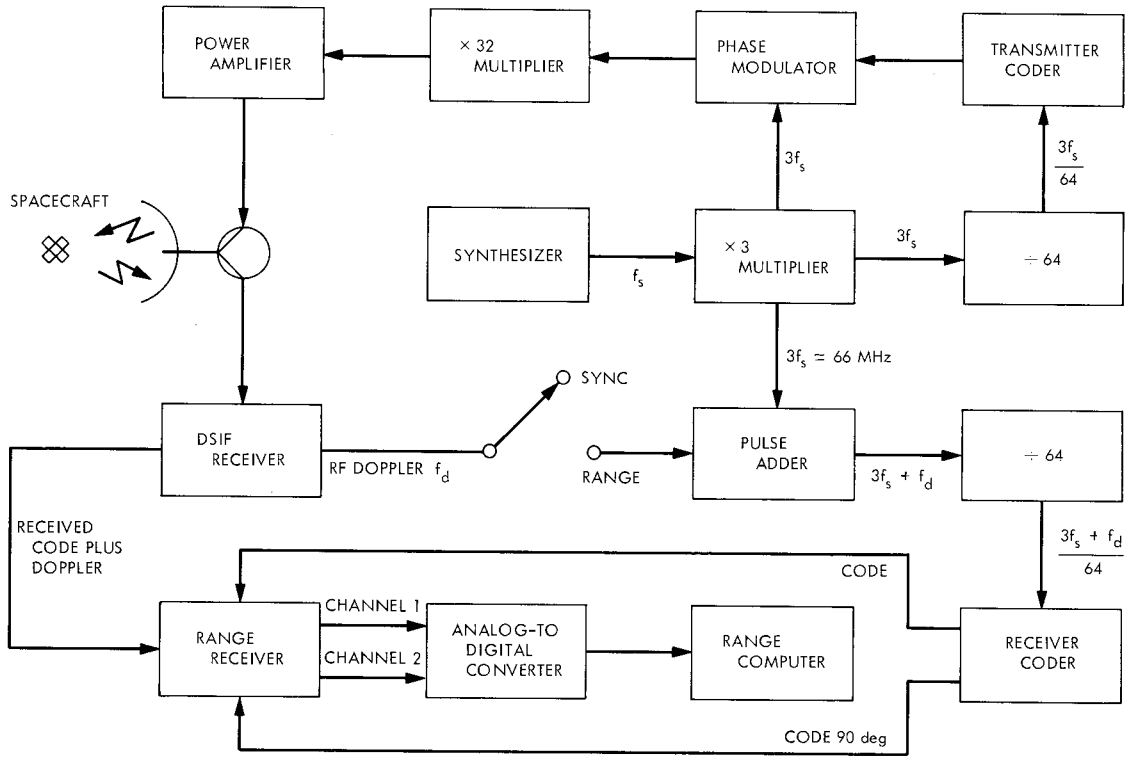

Fig. 43. Binary-coded sequential acquisition ranging system block diagram

the binary counter is individually selectable for modulating the transmitter. Thus, the period t_n of the nth component is given by

$$t_n = \frac{64 \times 2^n}{3 f_s} \qquad (2)$$

where f_s is the synthesizer's frequency.

From the above equation, it can be seen that the code's period is irrevocably tied to the transmitter's frequency. Changing the transmitter's frequency, as is done from time to time to assure optimum reception at the spacecraft, also changes the coder's frequency in direct proportion.

A virtually identical set of hardware exists in the receiver; however, the $\div 64$ is preceded by a doppler pulse adder circuit. The latter accepts as one of its inputs 66 MHz from the $\times 3$ multiplier in the transmitter chain. A second input connects RF doppler f_d, properly scaled, from the DSIF receiver. In the ranging mode, the output from the pulse adder circuit is the algebraic sum of the two inputs:

$$3 f_s + f_d$$

The receiver coder is a duplicate of its counterpart in the transmitter, except for the inclusion of a second output which provides code delayed by $\pi/2$. This second channel is combined with the first to establish the amplitude of the returning signal—a necessary step in measuring its phase.

When the range–sync switch is in sync position, the two coders will be operating synchronously. Because of the doppler frequency shift due to the relative motion of the spacecraft, the received signal will be slipping in phase with respect to the coders. If at some time t_0 the switch is changed to the range position, the receiver coder's frequency is instantly modified by the RF doppler and becomes coherent with the signal being received from the spacecraft. Assuming that the two coders have been synchronized prior to the changeover, the phase difference between the receiver coder and the incoming signal is a measure of range. Since this phase displacement is constant by virtue of the doppler rate aiding, the range measurement can be made at leisure.

Thus, a coherent model of the received signal is generated by modifying the frequency of the transmitted code with the spacecraft's doppler. Note that the tracking operation is open-loop, eliminating any settling time and

greatly simplifying the hardware design. Two conditions are necessary to make the scheme workable. First, before RF doppler can be used as a rate-aiding signal, the code must bear some simple, fixed relationship to the transmitted frequency. This is apparent from Eq. (2), which can be conveniently rewritten in terms of the transmitted frequency f_T,

$$t_n = \frac{2048}{f_T} \times 2^n \tag{3}$$

Second, mechanization required the availability of high-speed digital logic which could conveniently handle 66 MHz. Since the pulse adder serves to add or delete cycles from the 66-MHz reference, the logic must have a speed capacity well in excess of that frequency.

The question might well arise as to why such a high frequency was selected for the doppler addition. The answer can be best explained by an example. Consider a target whose distance is increasing at a uniform rate, resulting in a constant doppler frequency. Since the spacecraft is receding, the received frequency will be lower than that transmitted by the two-way doppler. Each doppler cycle detected by the DSIF receiver serves to delete one 66-MHz cycle in the pulse adder. Therefore, the receiver coder's phase will be delayed in a step-wise manner, resulting in a small phase jitter with respect to the incoming signal. The higher the frequency at which the doppler addition is done, the less the phase jitter.

The ranging receiver is shown in a simplified block diagram (Fig. 44). The input (from the DSIF receiver) consists of a 10-MHz carrier phase-modulated with code modified by two-way doppler. Two identical channels mix this signal with that from the receiver coder. The mixers are simple, rather inexpensive, diode switches which pass or invert the received signal, depending upon whether the local code is a 1 or a 0. When the receiver coder is in phase with the code returning from the spacecraft, the mixer's output will be a pure 10-MHz sine wave. Any phase displacement will result in a phase inversion of the sine wave. After amplification, a second identical mixer removes the 10 MHz, translating the received signal to baseband for further processing.

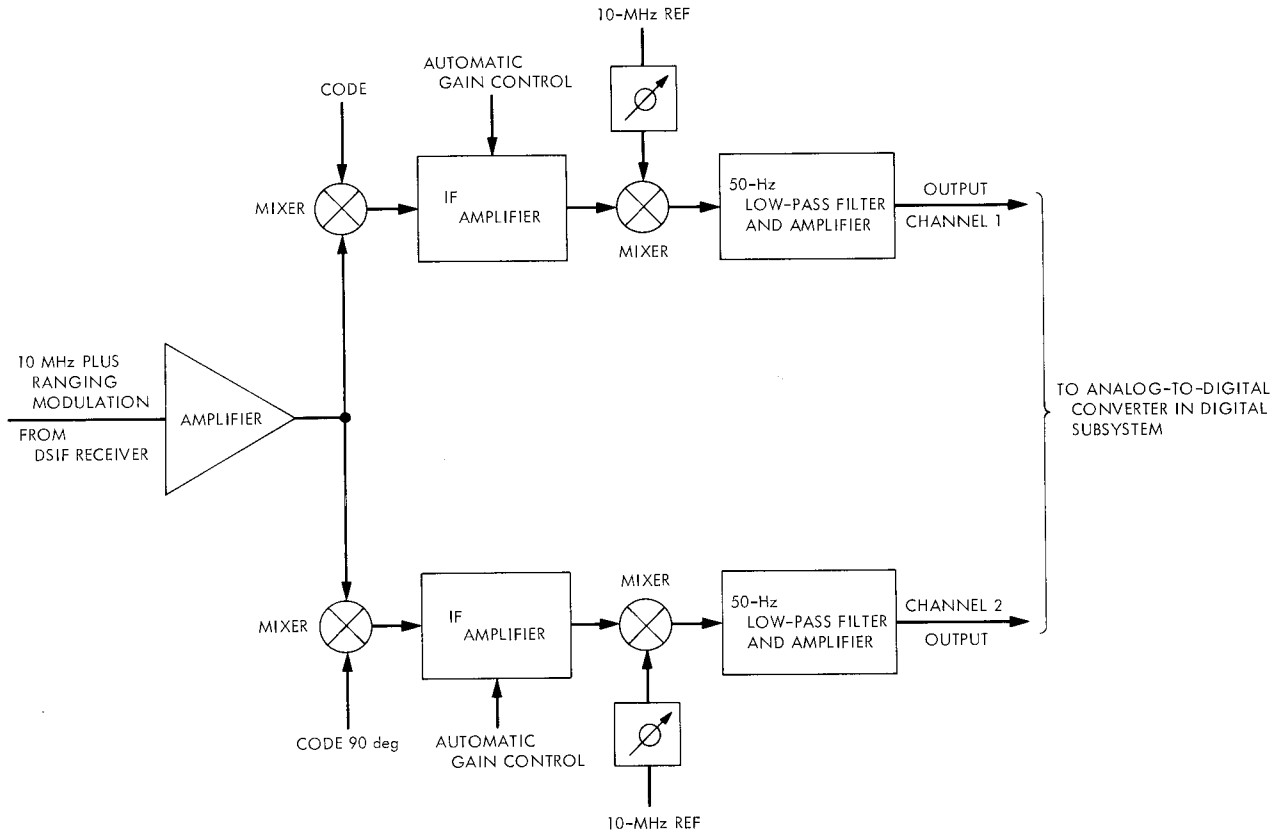

Fig. 44. Ranging receiver simplified block diagram

To eliminate effects due to dc drift or changes in amplification between the two channels, the code inputs are interchanged once per second. For example, if code is directed to channel 1 (CH 1), then code delayed by $\pi/2$ is used in channel 2 (CH 2). Coincident with the 1-s time tick, the inputs would be inverted so that not code and not code delayed by $\pi/2$ would be entered into channel 1 and channel 2, respectively. Again at the next 1-s tick, the two inputs would be exchanged and the procedure repeated until all four possible combinations were exhausted. The last two bits of the data input word specify the state of the code-channel assignment, allowing the computer to sort the data.

Table 11 describes the system's operation, which will be recognized as the exclusive *or* function. Figure 45 presents the same information graphically, showing the relative channel outputs as the phase is shifted between the received and local codes. A 12-bit analog-to-digital converter is used to measure channel amplitudes, and the result is transferred to a computer which calculates the phase displacement τ.

Table 11. Ranging receiver truth table

Received spacecraft code	Receiver coder	Ranging receiver output
0	0	+1
0	1	−1
1	0	−1
1	1	+1

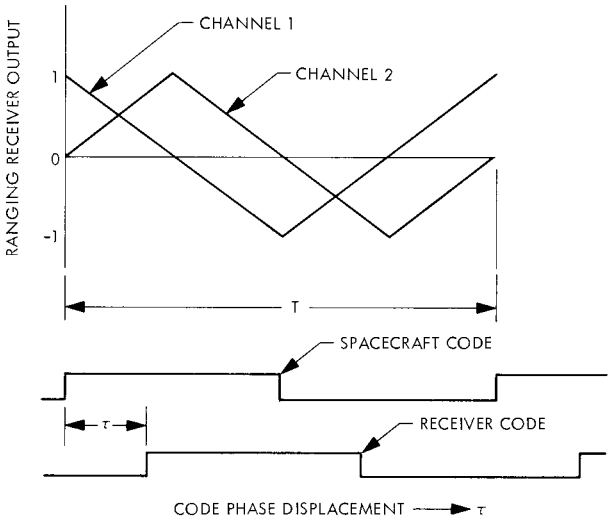

Fig. 45. Ranging receiver output characteristics

Two channels are required to measure the phase difference between the received code and that generated by the receiver coder. The method is analogous to the optimum phase estimator for sine waves. Both channels are sampled every 10 ms, and the results V_N are summed over some integration time t_i. After sufficient samples have been accumulated, the phase displacement can be computed using the relationship

$$\tau = \frac{\sum_{t=0}^{t_i} V_{\text{CH 1}}}{\left|\sum_{t=0}^{t_i} V_{\text{CH 1}}\right| + \left|\sum_{t=0}^{t_i} V_{\text{CH 2}}\right|} \times \frac{T}{4}, \qquad 0 < \tau < \frac{\pi}{2} \tag{4}$$

The above equation holds only for the first quadrant and similar expressions are necessary for the others. A summary of the respective equations is given in Table 12.

The highest frequency component, with a period of approximately 2 μs, provides the system's resolution. Unfortunately, any range measurement will have an ambiguity modulo of 2 μs, and a lower frequency code component must be used to resolve this uncertainty. Restated, the single function of all lower frequency

Table 12. Phase angle calculation

Phase displacement	Quadrant
$\tau = \left(\dfrac{\sum_{t=0}^{t_i} V_{\text{CH 1}}}{\left\lvert\sum_{t=0}^{t_i} V_{\text{CH 1}}\right\rvert + \left\lvert\sum_{t=0}^{t_i} V_{\text{CH 2}}\right\rvert} \right) \dfrac{T}{4}$	$0 < \tau < \dfrac{\pi}{2}$
$\tau = \left(2 - \dfrac{\sum_{t=0}^{t_i} V_{\text{CH 1}}}{\left\lvert\sum_{t=0}^{t_i} V_{\text{CH 1}}\right\rvert + \left\lvert\sum_{t=0}^{t_i} V_{\text{CH 2}}\right\rvert} \right) \dfrac{T}{4}$	$\dfrac{\pi}{2} < \tau < \pi$
$\tau = \left(2 + \dfrac{\sum_{t=0}^{t_i} V_{\text{CH 1}}}{\left\lvert\sum_{t=0}^{t_i} V_{\text{CH 1}}\right\rvert + \left\lvert\sum_{t=0}^{t_i} V_{\text{CH 2}}\right\rvert} \right) \dfrac{T}{4}$	$\pi < \tau < \dfrac{3\pi}{2}$
$\tau = \left(4 - \dfrac{\sum_{t=0}^{t_i} V_{\text{CH 1}}}{\left\lvert\sum_{t=0}^{t_i} V_{\text{CH 1}}\right\rvert + \left\lvert\sum_{t=0}^{t_i} V_{\text{CH 2}}\right\rvert} \right) \dfrac{T}{4}$	$\dfrac{3\pi}{2} < \tau < 2\pi$

components is simply to resolve the range ambiguity associated with the highest frequency code.

Eighteen code components have been designed into the system, the lowest frequency of which has a period of more than 0.25 s. The user is not required to employ all eighteen, but rather, should use only those necessary to resolve the range uncertainty. For example, if the range is known to within 1 ms (150 km), only the first ten components are required. Table 13 summarizes the range resolving capabilities of the various components.

Table 13. Code range resolving power

Component C_n	Approximate period t_{n_i}, μs	Approximate ambiguity resolving power, km
1	1.94	2.85×10^{-1}
2	3.88	5.70×10^{-1}
3	7.76	1.14
4	1.55×10^{1}	2.28
5	3.10×10^{1}	4.56
6	6.21×10^{1}	9.11
7	1.24×10^{2}	1.82×10^{1}
8	2.48×10^{2}	3.65×10^{1}
9	4.97×10^{2}	7.29×10^{1}
10	9.93×10^{2}	1.46×10^{2}
11	1.99×10^{3}	2.92×10^{2}
12	3.97×10^{3}	5.83×10^{2}
13	7.94×10^{3}	1.17×10^{3}
14	1.59×10^{4}	2.33×10^{3}
15	3.18×10^{4}	4.67×10^{3}
16	6.36×10^{4}	9.33×10^{3}
17	1.27×10^{5}	1.87×10^{4}
18	2.54×10^{5}	3.73×10^{4}

It has been shown by Goldstein (SPS 37-52, Vol. II, pp. 46–49) that a 3-dB improvement in system performance can be obtained by shifting the receiver coder to make $\tau = K(T/2)$ for $K = 1,2,3, \cdots, N$. This is equivalent to moving to a peak on the correlation function. Adopting the further constraint that the highest frequency code will always be shifted to make $\tau_1 = 0$ guarantees that the next lower code will also be at a peak (positive or negative). The procedure is best illustrated by a diagram.

Figure 46 shows the relative code correlation characteristics of the first three components. Suppose that the range to a target results in a $\tau = \tau_R$ (Fig. 46). Suppose further, that the range uncertainty $\hat{R}$ is in the interval

$$T_2 < \hat{R} < T_3$$

Measurement of code C_1 will indicate that the correlation amplitude is not at its peak value (i.e., $\tau_1 \neq 0$), and that a phase shift of the receiver coder is necessary. For simplicity of design, the shifting is accomplished by deleting coder drive pulses, in effect delaying the receiver coder. This is equivalent to reducing the target range and, of course, the value of τ. The high-frequency component is shifted by dropping 66-MHz cycles, resulting in a phase displacement of approximately 15 ns. A total of 128 shifts is required to slip the phase by one cycle.

After calculating the requisite number of shifts, the receiver coder is delayed to bring the correlation value to a positive peak, point Ⓐ, Fig. 46 (i.e., $\tau_1 = 0$). It is obvious from the diagram that now C_2 must also be at a peak, either positive or negative. Thus, when correlating with C_2, it is sufficient to determine the sign of the output without regard for magnitude. Had the result been positive, no shifting would be required. However, the measurement is clearly negative and a shift of $T_2/2$ is necessary to bring the component into alignment. This is accomplished by delaying C_2 by one-half cycle. All lower-order components will be shifted by the same amount. Having arrived at point Ⓑ, the procedure is repeated and C_3 is delayed by $T_3/2$ to reach point Ⓒ. The number of shifts required to reach point Ⓒ is a direct measure of the phase delay τ_R, and hence the range.

c. System performance. Thus far, the effect of noise in the received signal has not been considered. Its presence introduces a variance in the measured value of τ_R, which is a function of the integration time t_i. Two separate cases need to be examined. First, there is the highest frequency component C_1, which determines the system's accuracy and must be measured very carefully. Second, there are the remaining components, C_2 through C_{18}, which serve to resolve the ambiguity and need only a positive–negative determination.

A system analysis by Goldstein (SPS 37-52, Vol. II, pp. 46–49) has shown that the integration time required to achieve an acceptable variance σ_τ^2 is given by

$$t_i = \frac{T^2 N_o}{32 \sigma_\tau^2 s} \tag{5}$$

where s is the power in the ranging signal. Assuming that an uncertainty of ±15 m would be acceptable, and employing component C_1, Eq. (5) simplifies to

$$t_i = 12.5 \frac{N_o}{s} \tag{6}$$

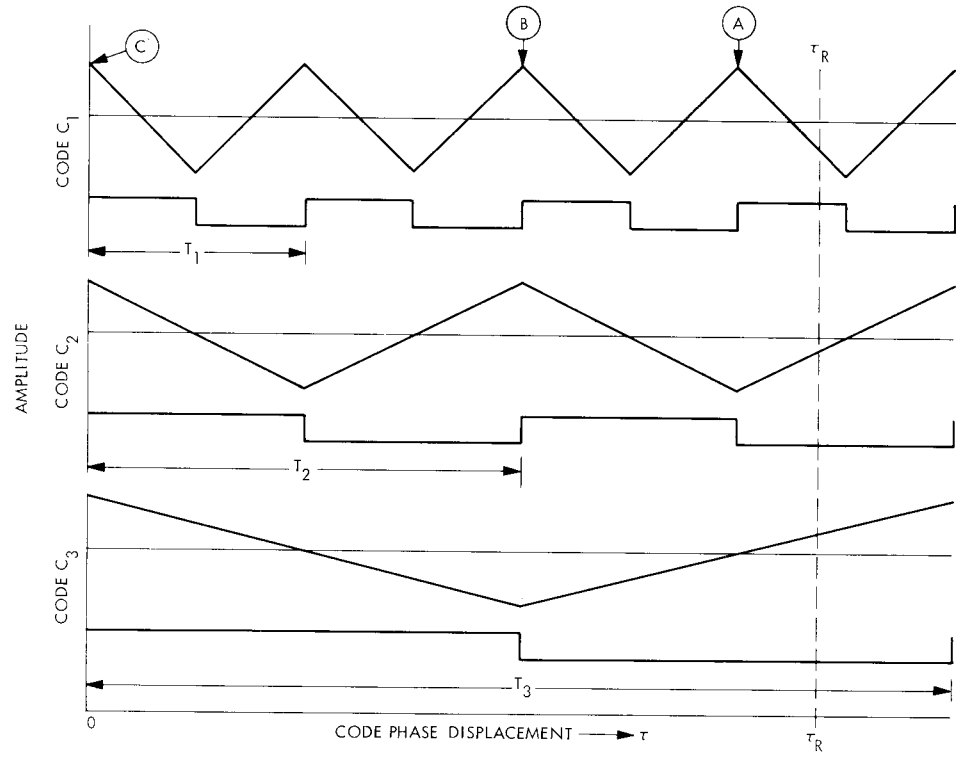

Fig. 46. Relative code correlation characteristics

This result is plotted in Fig. 47 for several values of s/N_o.

For the remaining components, C_2 through C_{18}, the probability of correctly identifying the phase is (SPS 37-52, Vol. III, pp. 46–49):

$$p\,(\text{correct}) = \frac{1}{\tau^{1/2}} \int_{-\infty}^{(st/N_o)^{1/2}} -e^{-Z^2}\,dz \qquad (7)$$

If an error is made in determining the phase of any component during the acquisition process, the entire range measurement will be incorrect. The probability of this occurring can be expressed as

$$P_e = 1 - p(\text{correct})^{n-1} \qquad (8)$$

Figure 48 graphically depicts the probability of error in resolving the code ambiguities. Curves for three different values of range uncertainties are shown which affect the number of components used. Thus, knowing the range uncertainty $\hat{R}$ and the expected s/N_o, the user can easily find the acquisition time t_a of all components except C_1. Total acquisition time is found by summing this result with t_{i_1}, found from Fig. 47.

d. Peripheral equipment.

Computer. In addition to the standard DSIF transmitter and receiver, a computer is required to control the equipment and to calculate the range. Since Scientific Data Systems series 920 computers are already installed in all tracking stations, it was decided to utilize these as part of the ranging equipment.

Programming inputs include the integration times for the first and other components, the number of components to be used, and the time to begin the transmission of C_1. Also, an estimate of the signal's round trip time-of-flight is required. The computer then calculates a set of critical times and stores them in a table which is constantly scanned during a ranging operation. These times specify the beginning and end of each component transmission and the times during which individual components should be available at the receiver for correlation. When a critical time is reached, a command is sent to the ranging equipment to instigate the appropriate action. A guard band of 1–2 s is left between critical times to allow for an uncertainty in the time-of-flight.

Transponder. A design constraint required the ranging equipment to be compatible with existing spacecraft

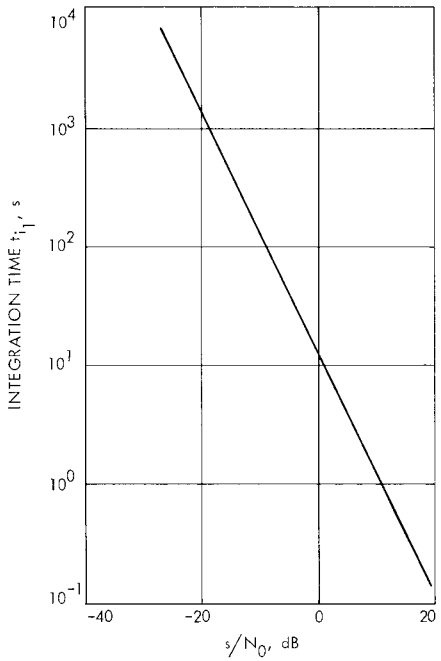

Fig. 47. Integration time t_{i_1}, first component for ± 15-m accuracy

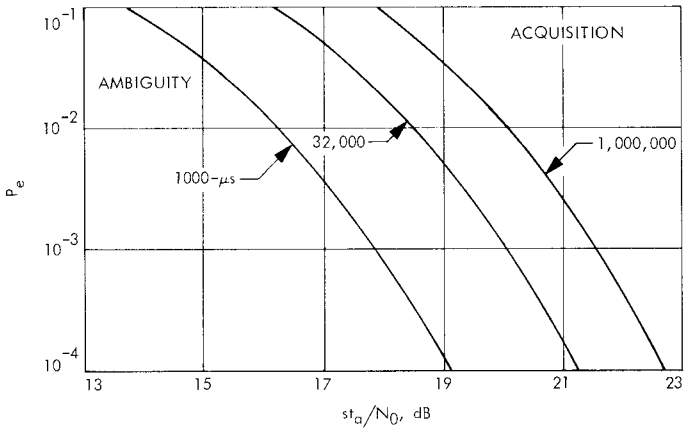

Fig. 48. Probability of an error in resolving the code ambiguities

transponders. The turnaround transponder detects and removes ranging modulation from the received carrier, which is then multiplied in frequency by 240/221. The new carrier is remodulated with the previously detected code and retransmitted to the ground station. Since present transponders have a bandwidth of about 3.5 MHz, the high-frequency code component must have a bit period of at least 1 μs.

Although turnaround transponders perform adequately on missions to Venus and Mars, very deep space probes where the signal level is weak may necessitate additional processing in the spacecraft. In these cases, a regenerative transponder which literally locks to and reconstructs the ranging code is essential. Regenerative ranging transponders for PN-encoded signals become rather complex devices. Not only are there n coders for an n component sequence, but also these must be individually locked to the received signal. In short, the spacecraft must execute an acquisition procedure identical to that of the ground equipment—a formidable task for something 500,000,000 mi away.

Unfortunately, code acquisition is required of all regenerative transponders, and the best one can hope for is to simplify the process. In this respect, square-wave codes, harmonically related by a factor of two and executed in a known and consistent manner, seem to offer a decided advantage. This advantage derives in part from the possibility of constructing a tracking filter (phase-locked loop) which can acquire the ranging modulation. By utilizing two such devices and associated lock detectors, the system could be tracking one component while simultaneously waiting for the next. Studies are under way to investigate the feasibility of such a design, which would make a regenerative transponder practical for the first time.

e. Ranging operation. Having considered the system's component parts in detail, it would be worthwhile to describe a typical ranging operation. Assume that the range to a spacecraft is $1.5 \times 10^6 \pm 100$ km and that the received $s/N_o = -10$ dB. The objective is to refine the range measurement to ±15 m with a $p_e = 10^{-4}$.

From Fig. 47, the integration time required for the first component is

$$t_i = 125 \text{ s}$$

Figure 48 shows the acquisition time for the remaining 9 components to be a total of 800 or 88.8 s each. These numbers, together with the test starting time, are entered into the computer, which then calculates the critical time table.

The computer then enters a wait phase, where it stays until the first critical time is reached, at which point transmission of component C_1 commences for a period t_{i_1}. Since the round trip time-of-flight will be 10 min, the first six components and part of the seventh can be transmitted before C_1 returns from the spacecraft. Just after its arrival, the computer disables the doppler rate

aiding, commands the receiver coder to generate component C_1, and synchronizes the receiver coder and its $\div 64$ driver with their counterparts in the transmitter chain. Coincident with the second 1-s time tick following coder synchronization, the doppler rate aiding will be enabled and an interrupt generated that causes the computer to read the time of day. It is at this time t_0 that the range measurement will be valid since this is the instant that the relationship between the receiver coder and the incoming signal becomes fixed.

The computer samples both channels every 10 ms for a period t_{i_1}. It then calculates the phase displacement τ_1 and shifts the receiver coder to reach a positive peak on the correlation curve. The procedure is repeated for the lower frequency components until all have been completed and the final value of τ_R can be computed.

When the time was reached for the transmission of the 10th component, the computer, at the user's option, could have commanded a chopper frequency. The system is designed so that any one of the six higher frequency components can be used to chop the lower nine. Operation is defined by

$$C_{1\text{-}6} \oplus C_{10\text{-}18} \tag{9}$$

where $\oplus$ denotes modulo two. This feature was included because ranging components below 1 kHz may interfere with the command decoding subsystem on some spacecraft.

After all components have been acquired, the user may wish to return to C_1 to further refine the range measurement. It must be understood, however, that no matter how long the operation is continued the output will be a single range valid at t_0. To obtain a new range number, the acquisition procedure must be repeated.

f. System errors. In addition to errors due to noise, which were discussed in *Paragraph c*, there are other sources, including the ground equipment, the spacecraft's transponder, and charged particle effects. These uncertainties are important only insofar as they cannot be measured and, hence, removed from the range determination.

The ground equipment is calibrated by actually ranging a target at a known distance. The difference between measured and surveyed range is due to system delay and must be subtracted from any measured range. Since the test is simple and the equipment is close at hand, the calibration can be done daily, if desired. Practically, the system has been designed to have a minimum delay, thus any changes are likely to be negligible.

The biggest problems are to be found in the transponder. Before launch, the system delay is measured as a function of temperature and signal level. Though these tests are meticulously made, once the spacecraft has been launched there is no way to repeat the calibration nor to check the device's stability. Some insight into the magnitude of this error can be gained from studying the calibration data. First, the total delay for recent units seems to be on the order of 1μs. Moreover, the change in delay over realistic temperature and signal levels has been less than 75 ns. These values correspond to 150 and 11 m of range, respectively. Ignoring long-term drift, which has not been shown to be a problem, the latter number should represent an upper bound on the uncertainty for the transponder. Both temperature and signal level are available in the telemetry data and can be used to apply corrections for increased accuracy, if the user desires.

A second problem arises due to spacecraft bandpass limitations. Its effect will be a slight distortion of component C_1, which results in a rounding of the correlation curve peaks (Fig. 46) at $KT/4$ for $K = 1,2,3,4$. The degree of distortion can be calculated and an appropriate correction applied, if desired.

The final source of errors, charged particles, is likely to be so small that it can be ignored in most instances. It occurs because the doppler rate aiding for the receiver coder is generated by dividing RF doppler. Restated, RF doppler is used to simulate code doppler by appropriate scaling. In the presence of charged particles, the two dopplers will be shifted in frequency in opposing directions, causing the receiver coder to slowly drift off the correlation peak. Recent studies show the range variation to be between 1–4 m at zenith and about four times that amount when the antenna is pointed toward the horizon.

g. System construction. In packaging the system, both the relative simplicity and the high frequencies involved suggested a small physical size. Furthermore, if this was a prototype for future DSN ranging equipment, then reliability would also be important. These things considered, mechanization with integrated circuits was mandatory, and Motorola's MECL II was selected for the digital portion. Emitter coupler logic offers the advantage of very high-speed (120-MHz), small propagation delays (2–4 ns) and a relatively constant power drain. Fourteen

lead flat packs were selected over dual-in-line packs because of an inherent size advantage.

A scheme was sought to mount the integrated circuits which would preserve both flexibility and space. Several methods were evaluated, but one developed by JPL and marketed by Microtechnology Corp., Canoga Park, Calif., seemed considerably better than the rest.

The basic unit consists of an etched circuit board on which are mounted 20 integrated circuits (Fig. 49). Twenty-two test points and forty-four connector pins serve to bring relevant signals to and from the outside world. Because of the high packing density, it is possible to make each card a complete, functional unit. For example, the device shown in Fig. 49 is a 9-stage coder with associated select gating, word detector, and a quadrature clock generator. Four of these cards, all identical, are required to mechanize the transmitter and receiver coders. A total of 20 cards are utilized in the digital portion of the ranging equipment, providing space for over 300 integrated circuits.

Figure 50 shows the interconnection side of the card. Number-30-gage, teflon-insulated, nickel wire is welded to stainless steel posts, which in turn are soldered to the leads of the integrated circuits. This method combines the inherent reliability of welded connections with the flexibility of an individually tailored card.

The digital subsystem and ranging receiver are each contained in a 7-in. slide-out drawer, which is 18 in. deep. Thus, the entire system, exclusive of DSIF equipment, occupies a volume of less than 3 ft^3.

h. Conclusions. This article has described a ranging system designed to extend the threshold to weaker signals without sacrificing the present high level of accuracy. The system employs up to 18 sequentially transmitted square-wave components with periods from 2 μs to 0.25 s. Unlike previous ranging equipment, the system is open loop and uses received doppler, properly scaled, to establish the incoming symbol rate. High-frequency digital logic, operating at decision rates on the order of 4 ns, is used for implementation. Total system size

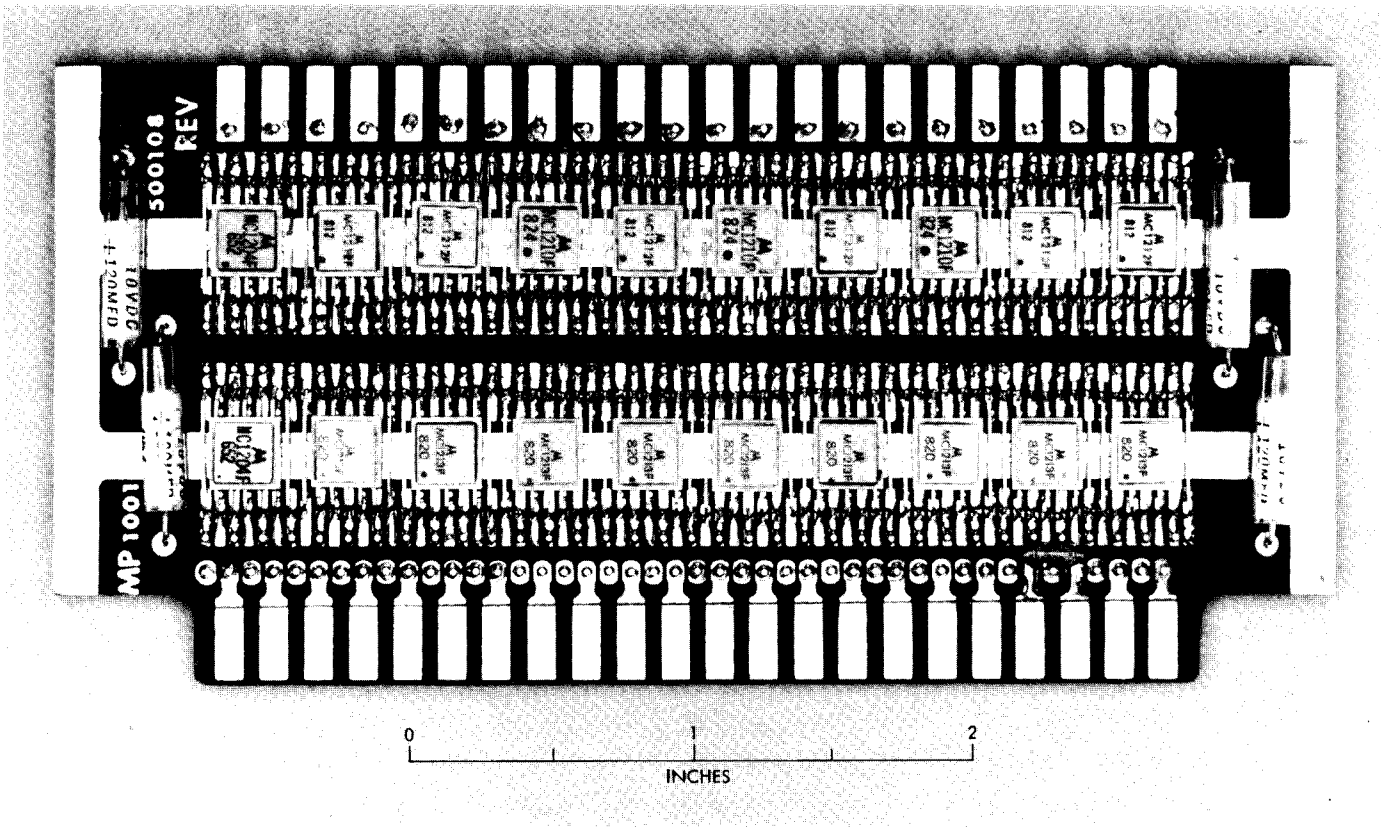

Fig. 49. Binary-coded sequential acquisition ranging system

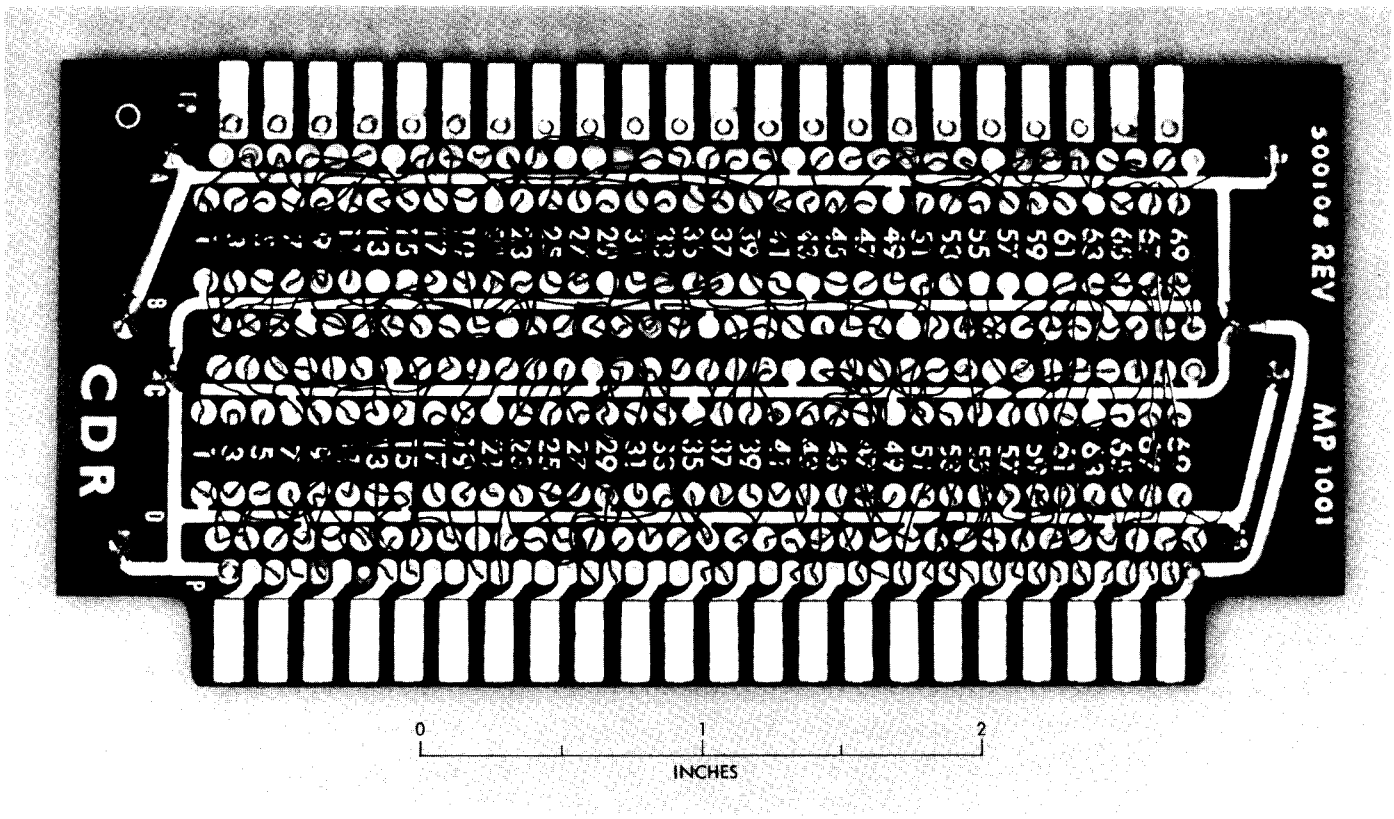

Fig. 50. Interconnection side of ranging system card

is less than 3 ft^3. A simplified transponder for use on very deep space probes is currently under investigation. The system is presently undergoing performance tests with the intent that it will be tried on *Mariner VI* and *VII* at some future date.

Reference

1. Titsworth, R. C., *Optimal Ranging Codes*, Technical Report 32-411. Jet Propulsion Laboratory, Pasadena, Calif., Apr. 15, 1963.

3. Communication Statistics: Estimation of the Parameters of the Distribution of Failure Time When the Effects of Chance and Wearout Are Combined,

I. Eisenberger

a. Introduction. The ultimate object of this work is to provide a better method of failure reporting and a more effective reliability policy for the DSIF.

For a certain period of time during the operating life of an electronic device or subsystem, failures are usually due entirely to chance occurrences. The distribution of failure time during this period for a single device is adequately described by the density function given by

$$f_1(t) = \lambda \exp(-\lambda t), \qquad t > 0$$

where λ is called the *failure rate.*

The distribution function, the probability of failure before time t, is given by

$$F_1(t) = 1 - \exp(-\lambda t)$$

Because this distribution has the property that the probability of failure between times t_1 and t_2, given that the device has survived until time t_1, depends only on the difference $t_2 - t_1$, the expected value of t, $1/\lambda$, is referred to as the *mean time between failures.* This means that if a device has survived to time t_o, the probability of failure between times t_o and $t_o + t$ is still $1 - \exp(-\lambda t)$. To show this, let T denote the time of operation from time zero. Then the probability of failure between $T = t_o$ and $T = t_o + t$, given that failure did not